Journal of Advanced Research (2015) 6, 203–217

Cairo University

Journal of Advanced Research

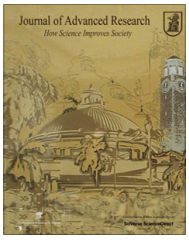

ORIGINAL ARTICLE

# Theoretical and experimental studies on the corrosion inhibition potentials of some purines for aluminum in 0.1 M HCl

**Nnabuk O. Eddy [a,*], H. Momoh-Yahaya [b], Emeka E. Oguzie [c]**

[a] *Department of Chemistry, Ahmadu Bello University, Zaria, Kaduna State, Nigeria*
[b] *Department of Chemistry, University of Agriculture Makurdi, P.M.B. 2373, Makurdi, Nigeria*
[c] *Electrochemistry and Materials Science Research Laboratory, Department of Chemistry, Federal University of Technology Owerri, P.M.B. 1526, Owerri, Nigeria*

ARTICLE INFO

*Article history:*
Received 25 August 2013
Received in revised form 8 January 2014
Accepted 9 January 2014
Available online 20 January 2014

*Keywords:*
Corrosion
Inhibition
Purines
Quantum chemical studies

ABSTRACT

Experimental aspect of the corrosion inhibition potential of adenine (AD), guanine (GU) and, hypoxanthine (HYP) was carried out using weight loss, potentiodynamic polarization and electrochemical impedance spectroscopy (EIS) methods while the theoretical aspect of the work was carried out by calculations of semi-empirical parameters (for AM1, MNDO, CNDO, PM3 and RM1 Hamiltonians), Fukui functions and inhibitor–metal interaction energies. Results obtained from the experimental studies were in good agreement and indicated that adenine (AD), guanine (GU) and hypoxanthine (HYP) are good adsorption inhibitors for the corrosion of aluminum in solutions of HCl. Data obtained from electrochemical experiment revealed that the studied purines functioned by adsorption on the aluminum/HCl interface and inhibited the cathodic half reaction to a greater extent and anodic half reaction to a lesser extent. The adsorption of the purines on the metal surface was found to be exothermic and spontaneous. Deviation of the adsorption characteristics of the studied purines from the Langmuir adsorption model was compensated by the fitness of Flory Huggins and El Awardy et al. adsorption models. Quantum chemical studies revealed that the experimental inhibition efficiencies of the studied purines are functions of some quantum chemical parameters including total energy of the molecules (TE), energy gap ($E_{L-H}$), electronic energy of the molecule (EE), dipole moment and core–core repulsion energy (CCR). Fukui functions analysis through DFT and MP2 theories indicated slight complications and unphysical results. However, results obtained from calculated Huckel charges, molecular orbital and interaction energies, the adsorption of the inhibitors proceeded through the imine nitrogen (N5) in GU, emanine nitrogen (N7) in AD and the pyridine nitrogen (N5) in HPY.



* Corresponding author. Tel.: +234 8038198753.
E-mail address: nabukeddy@yahoo.com (N.O. Eddy).
Peer review under responsibility of Cairo University.

Production and hosting by Elsevier

## Introduction

Industrial revolution that is ever expanding within different parts of the world has several advantages and disadvantages in the quality of environment. Most industries utilize metals or their ores (such as mild steel, aluminum, zinc, and copper)

2090-1232 © 2014 Production and hosting by Elsevier B.V. on behalf of Cairo University.
http://dx.doi.org/10.1016/j.jare.2014.01.004

in the fabrication of their installations. In most cases, these metals are exposed to aggressive medium/media and are prone to corrosion [1]. Corrosion is an electrochemical process that gradually returns the metal to its natural state in the environment. Corrosion in industries is often activated by processes such as acid wash, etching, prickling and others. Aluminum owes its widespread use after steel, to its excellent corrosion resistance to the air formed film strongly bonded to its surface. This film is relatively stable in aqueous solutions over a pH range of 4–8.5 [2]. In such solutions the surface film is insoluble but may be locally attacked by aggressive anions, primarily chlorides. The effect of $Cl^-$ ions (which can be generated by hydrolysis of HCl) on the corrosion of aluminum and its alloys has been the subject of several studies [3–5]. The cost of replacing metals due to corrosion is often exorbitant and economically unbearable. Therefore, industries have adopted several options to control corrosion of metals including anodic/cathodic protection, painting, electroplating and galvanizing. However, the use of corrosion inhibitors has proven to be one of the most effective methods.

Inhibitors are compounds that retard the rate of corrosion of metals by been absorbed on the surface of the metal either through the transfer of charge from charge inhibitor molecule to charged metal surface (physical adsorption) or by electron transfer from the inhibitor's molecule to the vacant d-orbital of the metal(chemical adsorption) [6]. Numerous studies have been carried out on the corrosion of metals in different environments and most of the well-known and suitable inhibitors are heterocyclic compounds [7–10]. For these compounds, their adsorption on the metal surface is the initial step of inhibition [11,12]. The adsorption of inhibitor is linked to the presence of heteroatoms (such as N, O, P, and S) and long carbon chain length as well as triple bond or aromatic ring in their molecular structure [13]. Generally, a strong coordination bond leads to higher inhibition efficiency. The corrosion inhibition potentials of some purines and their derivatives have been reported by several researchers [14–19].

Although quantum chemical studies limits the corrosion inhibition efficiency with molecular orbital energy levels of some organic compounds, semi-empirical method emphasizes the approaches that are involved in the selection of inhibitor by correlating the experimental data with quantum chemical properties such as energy of the highest molecular orbital ($E_{HOMO}$), the energy of the lowest unoccupied molecular orbital ($E_{LUMO}$), total negative charge (TNC), electronic energy (EE), binding energy ($E_b$), core–core repulsion energy (CCR), dipole moment and other parameters [20,21]. Also, the use of Fukui functions, calculated through Milliken, Lowdin or Hierfield charges have proven to be very useful in predicting the sites for electrophilic and nucleophilic attacks.

The present study is aimed at investigating the inhibitory and adsorption properties of some purines, namely (AD), guanine (GU) and hypoxanthine (HYP) for the corrosion of aluminum in HCl using gravimetric, electrochemical and quantum chemical methods.

## Experimental

### *Material*

Aluminum sheet (AA 1060 type) and purity 98.5% was used in this study. Acid solution of 0.1 M HCl was prepared by diluting analytical grade with distilled water. Various concentrations (ranging from $2.0 \times 10^{-3}$ to $10.0 \times 10^{-3}$ M) of the inhibitors were also prepared in the acid media. All reagents were obtained from Zayo-Sigma Chemicals. Fig. 1 shows chemical structures of adenine (AD), guanine (GU) and hypoxanthine (HYP).

### *Experimental procedure*

#### *Weight loss measurements*

Aluminum coupons of dimension $5.0 \times 4.0 \times 0.15$ cm were cut and wet-abraded with silicon carbide abrasive paper (from grade #1000 to #1200), rinsed with distilled water and in acetone before they were dried in the air. The pre-cleaned and weighed coupons were suspended in beakers containing the test solutions using glass hooks and rods. Tests were conducted under total immersion conditions in 150 mL of the aerated and unstirred test solutions. Immersion time was varied from 1 to 5 days (120 h) in 0.1 M HCl. The coupons were retrieved from test

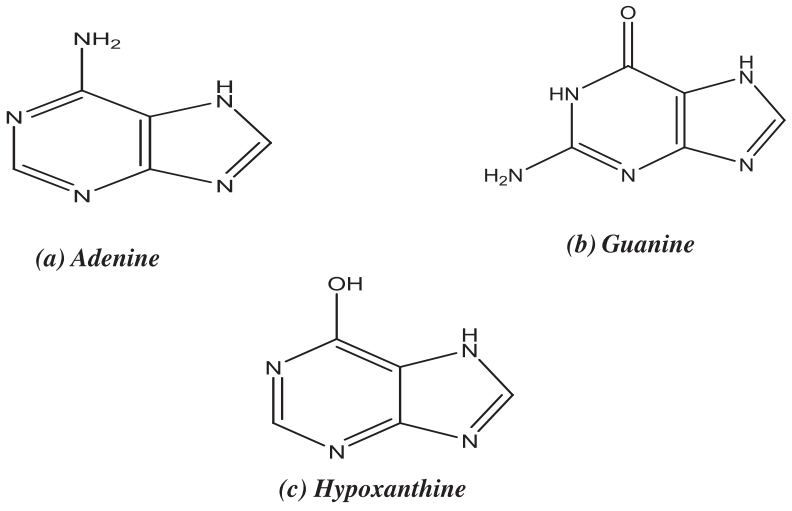


**Fig. 1** Molecular structures of (a) adenine (b) guanine and (c) hypoxanthine.

**Table 1** Corrosion rates of aluminum and inhibition efficiencies of adenine (AD), guanine (GU) and hypoxanthine (HYP) at 303 and 333 K respectively, in 0.1 M HCl.

| Inhibitor | C (M) | Corrosion rate $\times 10^{-4}$ (g $h^{-1}$ $cm^{-2}$) | | Inhibition efficiency (IE%) | |
|---|---|---|---|---|---|
| | | 303 K | 333 K | 303 K | 333 K |
| | Blank | 1.26 | 8.11 | – | – |
| AD | 0.002 | 0.356 | 4.20 | 71.73 | 48.27 |
| | 0.004 | 0.306 | 3.51 | 75.70 | 56.74 |
| | 0.006 | 0.233 | 3.21 | 81.49 | 60.41 |
| | 0.008 | 0.173 | 2.49 | 86.28 | 69.29 |
| | 0.01 | 0.119 | 2.23 | 90.58 | 72.58 |
| GU | 0.002 | 0.231 | 3.06 | 81.65 | 62.28 |
| | 0.004 | 0.177 | 2.74 | 85.95 | 66.26 |
| | 0.006 | 0.127 | 2.52 | 89.92 | 68.91 |
| | 0.008 | 0.090 | 2.43 | 92.89 | 70.06 |
| | 0.01 | 0.044 | 2.15 | 96.53 | 73.50 |
| HYP | 0.002 | 0.216 | 3.59 | 82.84 | 55.79 |
| | 0.004 | 0.17 | 3.22 | 86.54 | 60.36 |
| | 0.006 | 0.136 | 2.85 | 89.22 | 64.88 |
| | 0.008 | 0.117 | 2.61 | 90.72 | 67.83 |
| | 0.01 | 0.098 | 2.35 | 92.23 | 71.01 |

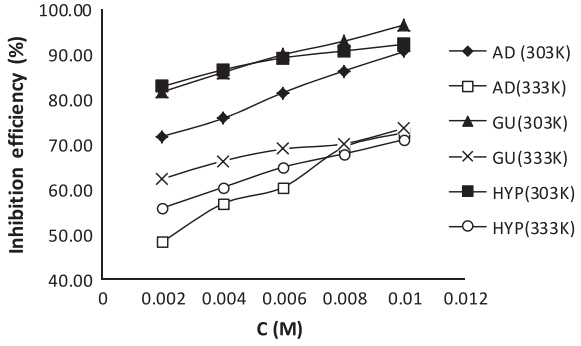


**Fig. 2** Variation of inhibition efficiency with concentration for AD, GU and HPY for the corrosion of aluminum in 0.1 M HCl at 303 and 333 K.

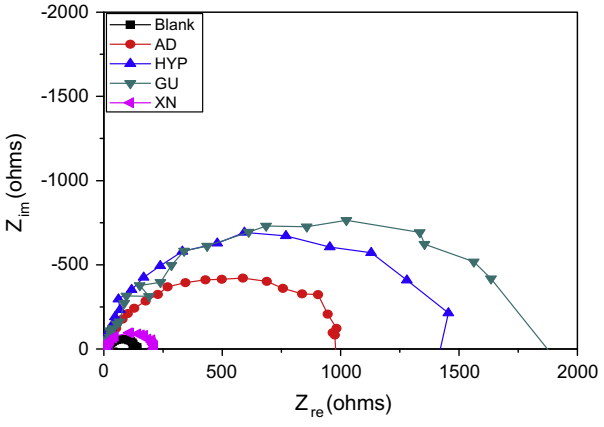


**Fig. 3** Electrochemical impedance spectra of aluminum in 0.1 M solutions of HCl in the absence and presence of 0.01 M AD, GU and HYP at 303 K.

solutions after every 24 h, appropriately cleaned, dried and re-weighed. The weight loss was taken to be the difference between the weight of the coupons at a given time and its initial weight. The effect of temperature on Al corrosion and corrosion inhibition was investigated by repeating the experiments at 303 and 333 K respectively. All tests were run in duplicate and the data obtained showed good reproducibility.

*Electrochemical measurements*

Metal samples for electrochemical experiments were machined into test electrodes of dimension $1.0 \times 1.0$ $cm^2$ and sealed with epoxy resin in such a way that only one square surface area (1 $cm^2$) was left uncovered. The exposed surface was cleaned using the procedure described above. Electrochemical tests were conducted in a Model K0047 corrosion cell using a VERSASTAT 400 complete DC voltammetry and corrosion system, with V3 Studio software. A graphite rod was used as a counter electrode and a saturated calomel electrode (SCE) as a reference electrode. The latter was connected via a Luggin capillary. Measurements were performed in aerated and unstirred solutions at the end of 1 h of immersion at 303 K. Impedance measurements were made at corrosion potentials ($E_{corr}$) over a frequency range of 100 kHz–10 mHz, with a signal amplitude perturbation of 5 mV. Potentiodynamic polarization studies were carried out in the potential ranging from −1000 to 2000 mV versus corrosion potential at a scan rate of 0.33 mV/s. Each test was run in triplicate [22].

*Quantum chemical calculations*

Full geometric optimization of each of the studied purines was carried out using molecular mechanics, ab ignition and DFT level of theories in the HyperChem release 8.0 software. Semi-empirical parameters were calculated using optimized structure of each of the purines as an input to the MOPAC software, while Muliken and Lowdin charges were calculated using GAMMES software. All quantum chemical calculations were carried out on gas phase.

**Table 2** Impedance and polarization data for aluminum in 0.1 mol $dm^{-3}$ HCl in the absence and presence of 0.01 mol $dm^{-3}$ adenine (AD), guanine (GU) and hypoxanthine (HYP) at 303 K.

| System | Impedance | | | | Polarization | | |
|---|---|---|---|---|---|---|---|
| | $R_{ct}$ ($\Omega$ $cm^2$) | $C_{dl}$ ($\mu\Omega^{-1}$ $S^n$ $cm^{-2}$) | $N$ | IE% | $E_{corr}$ (mV versus SCE) | $i_{corr}$ ($\mu$A $cm^{-2}$) | IE% |
| Blank | 101.00 | 21.89 | 0.99 | – | −703.00 | 265.12 | – |
| AD | 907.00 | 3.72 | 0.92 | 88.87 | −685.93 | 29.56 | 88.85 |
| GU | 1756.52 | 2.51 | 0.91 | 94.25 | −707.72 | 14.93 | 94.37 |
| HYP | 1175.80 | 2.68 | 0.98 | 91.41 | −703.05 | 23.28 | 91.22 |

**Table 3** Langmuir, Flory Huggins and El Awardy et al. parameters for the adsorption of AD, GU and HPY on Al surface at 303 and 333 K.

| Isotherm | $T$ (K) | Slope | Intercept | $n/1/y$ | $\Delta G^0_{ads}$ (kJ/mol)/B | $R^2$ |
|---|---|---|---|---|---|---|
| Langmuir | AD (303 K) | 0.8545 | −0.2400 | | −8.73 | 0.9986 |
| | AD (333 K) | 0.7463 | −0.3632 | | −8.80 | 0.9972 |
| | GU (303 K) | 0.8982 | −0.183 | | −9.06 | 0.9997 |
| | GU (333 K) | 0.9032 | −0.0541 | | −10.77 | 0.9997 |
| | HPY (303 K) | 0.9332 | −0.0982 | | −9.55 | 1.0000 |
| | HPY (333 K) | 0.8505 | −0.1458 | | −10.19 | 0.9996 |
| Flory Huggins | AD (303 K) | 1.1246 | 3.0421 | 1 | −27.77 | 0.8392 |
| | AD (333 K) | 1.7446 | 2.8094 | 2 | −26.42 | 0.8930 |
| | GU (303 K) | 1.2798 | 3.4904 | 1 | −30.37 | 0.9289 |
| | GU (333 K) | 4.2163 | 4.2271 | 4 | −34.64 | 0.9411 |
| | HPY (303 K) | 1.8878 | 4.0206 | 2 | −33.44 | 0.9784 |
| | HPY (333 K) | 3.1649 | 3.5061 | 3 | −30.46 | 0.9520 |
| El Awardy et al. | AD (303 K) | 9.0275 | 25.803 | 0.1108 | −25.55 | 0.7581 |
| | AD (333 K) | 2.3778 | 7.1637 | 0.4206 | −29.02 | 0.8748 |
| | GU (303 K) | 13.356 | 39.577 | 0.0748 | −26.13 | 0.8568 |
| | GU (333 K) | 1.4599 | 5.5222 | 0.6850 | −33.71 | 0.9208 |
| | HPY (303 K) | 9.6585 | 30.287 | 0.1035 | −27.09 | 0.9332 |
| | HPY (333 K) | 1.6404 | 5.5832 | 0.6096 | −31.40 | 0.9334 |

$n$ is applicable to Flory Huggins while $1/y$ and $B$ are for El Awardy et al. adsorption isotherms.

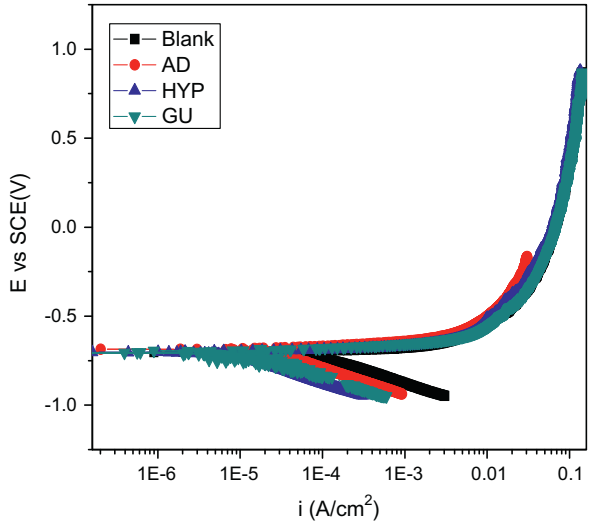


**Fig. 4** Polarization curves of aluminum in 0.1 M solutions of HCl in the absence and presence of 0.01 M AD, GU and HYP at 303 K.

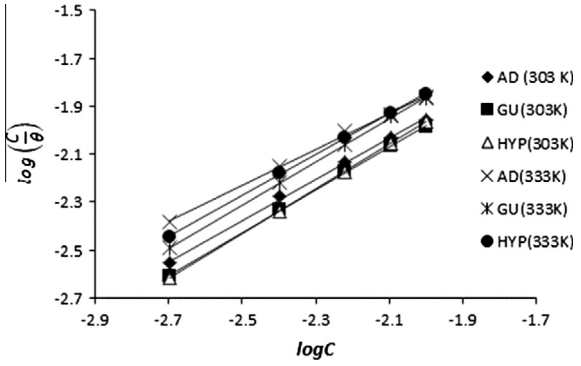


**Fig. 5** Langmuir isotherms for the adsorption of AD, GU and HPY onto Al surface at 303 and 333 K.

## Results and discussion

### *Weight loss measurements*

The corrosion rate, CR g $cm^{-2}$ $h^{-1}$ and inhibition efficiency, IE%, as functions of concentration in the acid media were calculated using the equation [23]:

**Table 4** Calculated values of activation energies ($E_a$) and heats of adsorption ($Q_{ads}$) for the corrosion of aluminum in 0.1 M HCl in the absence and presence of various concentrations of adenine (AD), guanine (GU) and hypoxanthine (HYP).

| Inhibitor | Concentration mol dm$^{-3}$ | Activation energy, $E_a$ (kJ mol$^{-1}$) | Heat of adsorption, $Q_{ads}$ (kJ mol$^{-1}$) |
|---|---|---|---|
| | Blank | 52.13 | |
| AD | 0.002 | 69.10 | −10.58 |
| | 0.004 | 68.31 | −9.15 |
| | 0.006 | 73.44 | −11.20 |
| | 0.008 | 74.66 | −10.84 |
| | 0.01 | 78.94 | −12.28 |
| GU | 0.002 | 72.34 | −10.48 |
| | 0.004 | 76.39 | −12.01 |
| | 0.006 | 77.46 | −14.72 |
| | 0.008 | 82.39 | −18.18 |
| | 0.01 | 84.55 | −24.37 |
| HYP | 0.002 | 78.69 | −14.19 |
| | 0.004 | 82.35 | −15.23 |
| | 0.006 | 85.18 | −15.86 |
| | 0.008 | 86.93 | −16.21 |
| | 0.01 | 88.98 | −16.69 |

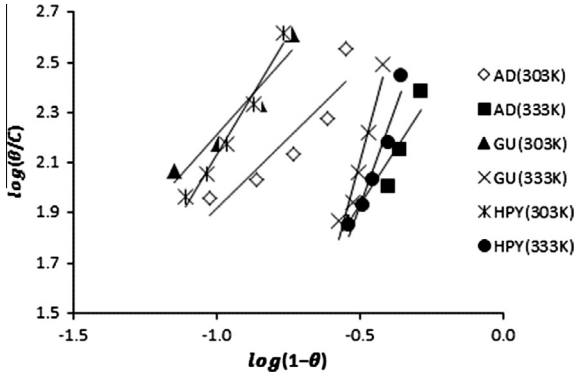


**Fig. 6** Flory Huggins isotherm for the adsorption of AD, GU and HPY on aluminum surface at 303 and 333 K.

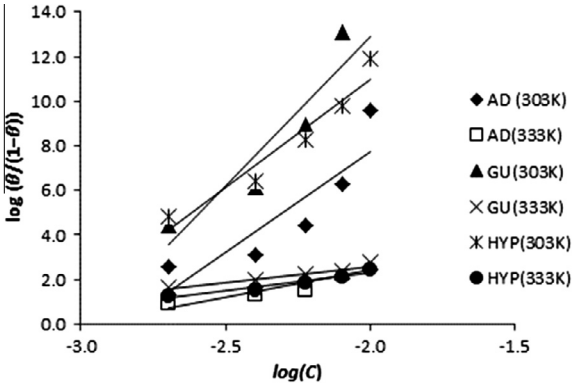


**Fig. 7** El awardy et al. isotherm for the adsorption of AD, GU and HPY on aluminum surface at 303 and 333 K.

$$\text{CR } (\text{g h}^{-1}\ \text{cm}^{-2}) = \frac{\Delta W}{At} \tag{1}$$

$$\text{IE}\% = \left(1 - \frac{\Delta W_{\text{inh}}}{\Delta W_{\text{blank}}}\right) \times 100 \tag{2}$$

where $\Delta W$ is the weight loss in g, $A$ is the surface area of the coupon and $t$ is the immersion time, $\Delta W_{\text{inh}}$ and $\Delta W_{\text{blank}}$ are the weight losses (g) of aluminum in the presence and absence of the inhibitor respectively. The results obtained are presented in Table 1.

Fig. 2 shows plots for the variation of IE% with concentration for AD, GU and HPY in 0.1 M HCl and at 303 and 333 K. The plots reveal that the inhibition efficiencies of the studied purines increase with increase in the concentration of the respective purine which suggest that the inhibition efficiency is a function of the amount of the inhibiting species present in the system and that the area of the aluminum surface covered by the adsorbed inhibitors is increased. Again, it is obvious from the plots that all the studied purines had high inhibition efficiencies with GU as the most effective inhibitor suggesting that not only the inhibitory power of the inhibitors increased with concentration but the performance also is a function of the type of purine.

*Electrochemical impedance spectroscopy*

Nyquist plots displayed in Fig. 3 revealed semicircles for all systems over the studied frequency range. The high frequency intercept with the real axis in the Nyquist plots is assigned to the solution resistance ($R_s$) and the low frequency intercept with the real axis is ascribed to the charge transfer resistance ($R_{ct}$).

The impedance spectra were analyzed by fitting information to the equivalent circuit model $R_s(Q_{dl}R_{ct})$. In this equivalent circuit, the solution resistance was shorted by a constant phase element (CPE) that is placed in parallel to the charge transfer resistance. The CPE is used in place of a capacitor to compensate for deviations from ideal dielectric behavior arising from the inhomogeneous nature of the electrode surfaces. The impedance of the CPE is given by [24];

$$Z_{\text{CPE}} = Q^{-1}(j\omega)^{-n} \tag{3}$$

**Table 5** Computed values of semi-empirical parameters for adenine, quinine and hypoxanthine.

| | CNDO | MNDO | AM1 | RM1 | PM3 |
|---|---|---|---|---|---|
| *$E_{HOMO}$ (eV)* | | | | | |
| Adenine | −11.430 | −9.591 | −9.511 | −9.424 | −9.062 |
| Quanine | −10.130 | −9.054 | −8.993 | −8.885 | −8.688 |
| Hypoxanthine | −11.577 | −9.876 | −9.851 | −9.811 | −9.596 |
| *$E_{LUMO}$ (eV)* | | | | | |
| Adenine | 3.520 | −0.102 | −0.021 | 0.137 | −0.263 |
| Quanine | 3.231 | −0.164 | −0.100 | 0.084 | −0.280 |
| Hypoxanthine | 2.776 | −0.665 | −0.583 | −0.509 | −0.800 |
| *$E_{L–H}$ (eV)* | | | | | |
| Adenine | 14.950 | 9.489 | 9.491 | 9.561 | 8.799 |
| Quanine | 13.361 | 8.890 | 8.892 | 8.968 | 8.408 |
| Hypoxanthine | 14.353 | 9.211 | 9.268 | 9.302 | 8.796 |
| *μ (Debye)* | | | | | |
| Adenine | 6.157 | 5.803 | 5.989 | 6.327 | 6.266 |
| Quanine | 3.747 | 2.170 | 2.322 | 2.482 | 2.491 |
| Hypoxanthine | 6.416 | 5.728 | 5.717 | 6.100 | 5.986 |
| *$E_b$ (eV)* | | | | | |
| Adenine | −221.16 | −69.17 | −67.54 | −71.12 | −69.31 |
| Quanine | −1555546.00 | −39442.70 | −1057934.00 | −38629.40 | −39568.00 |
| Hypoxanthine | −1385995.00 | −35667.00 | −34597.80 | −32733.40 | −35460.80 |
| *EE (eV)* | | | | | |
| Adenine | −9490.55 | −7789.66 | −7778.36 | −7779.22 | −7385.55 |
| Quanine | −6028329.00 | −4974777.00 | −4967677.00 | −4966004.00 | −4740755.00 |
| Hypoxanthine | −5158937 | −4222164.00 | −4215761.00 | −4212423.00 | −4021481.00 |
| *TE (eV)* | | | | | |
| Adenine | −2650.37 | −1741.59 | −1738.20 | −1741.78 | −1476.84 |
| Quanine | −1678629.00 | −1099277.00 | −1096446.00 | −1096585.00 | −943142.00 |
| Hypoxanthine | −113224.00 | −981435.00 | −978842.00 | −976977.00 | −848255.00 |
| *CCR (eV)* | | | | | |
| Adenine | 3,643,243 | 3,221,244 | 3,217,150 | 3,215,699 | 3,147,134 |
| Quanine | 4,349,700 | 3,875,500 | 3,871,231 | 3,869,402 | 3,797,613 |
| Hypoxanthine | 3,659,719 | 3,240,729 | 3,236,920 | 3,234,293 | 3,173,226 |

where $Q$ and $n$ represents the CPE constant and exponent respectively, $j = (-1)^{1/2}$ is an imaginary number, and $\omega$ is the angular frequency in rad $s^{-1}$ ($\omega = 2\pi f$), while f is the frequency in $Hz$.

The corresponding electrochemical parameters are presented in Table 2 and from the results obtained, it can be stated that the presence of AD, GU and HYP increases the magnitude of $R_{ct}$, with corresponding decrease in the double layer capacitance ($Q_{dl}$). The increase in $R_{ct}$ values in inhibited systems, which corresponded to an increase in the diameter of the Nyquist semicircle, confirms the corrosion inhibiting effect of the purines. The observed decrease in $C_{dl}$ values, which normally results in the double-layer thickness can be attributed to the adsorption of the purines (with lower dielectric constant compared to the displaced adsorbed water molecules) onto the aluminum/acid interface, thereby protecting the metal from corrosion.

Inhibition efficiency from the impedance data was estimated by comparing the values of the charge transfer resistance in the absence ($R_{ct}$) and presence of inhibitor ($R_{ct,inh}$) as follows [18]:

$$IE\% = \left(\frac{R_{ct(inh)} - R_{ct}}{R_{ct(inh)}}\right) \times 100 \quad (4)$$

The magnitude and trend of the obtained values presented in Table 3 are in close agreement with those determined from gravimetric measurements.

### *Potentiodynamic polarization data*

Polarization measurements were undertaken to investigate the behavior of aluminum electrodes in 0.1 M solutions of HCl in the absence and presence of the purines. The current–potential relationship for the aluminum electrode in various test solutions is shown in Fig. 4 while the electrochemical data obtained from the polarization curves are presented in Table 3.

Addition of the purines is seen to affect the cathodic partial reaction mostly, thereby reducing the cathodic current densities and the corresponding corrosion current density ($i_{corr}$). This indicates that the purines functioned as cathodic inhibitors for the corrosion of aluminum in 0.1 M HCl solutions. Adenine (AD) however, is also observed to affect the anodic arm of the Tafel plot, slightly, indicating that is functioned as a mixed inhibitor in 0.1 M HCl [11]. It was also seen that the potential range in the Tafel plots is short. This can be explained as follows. A typical Tafel plots will show Tafel region, plateau region and high polarization region. This study revealed the dominance of the Tafel region and thus a short

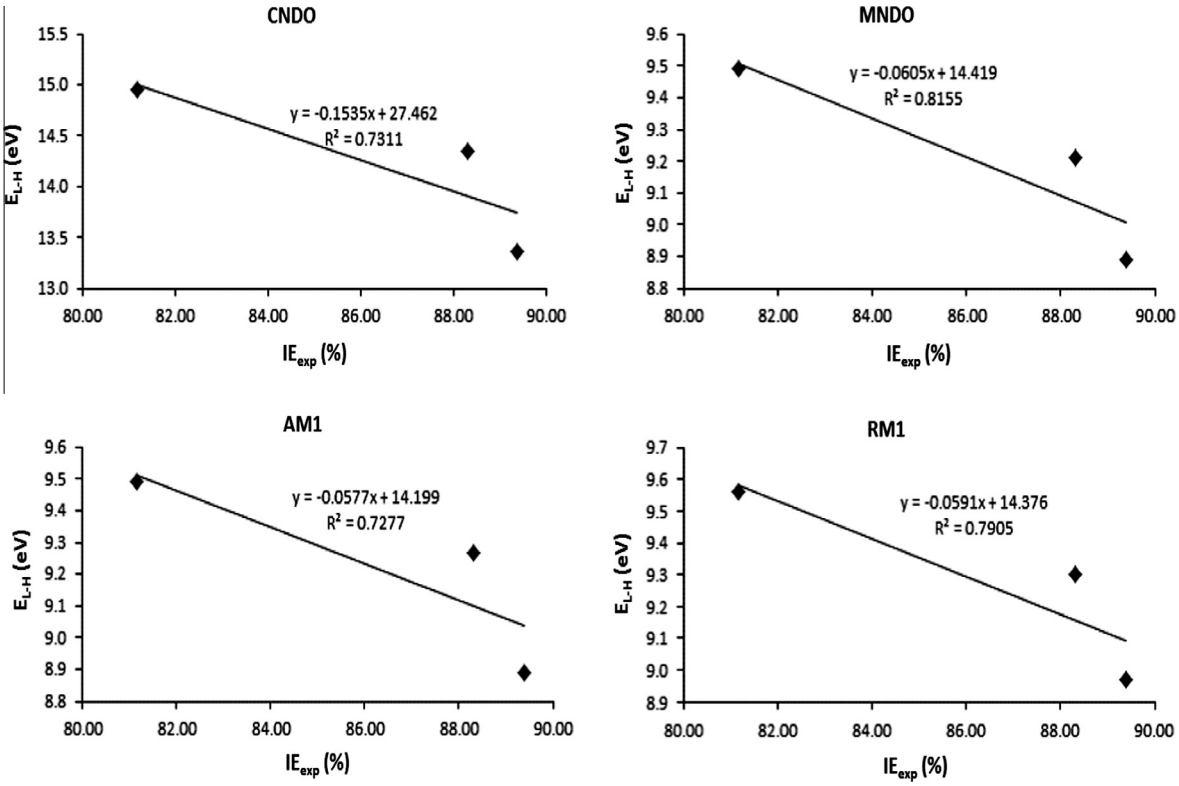


**Fig. 8** Variation of $E_{L-H}$ with experimental inhibition efficiencies of ADN, GUN and HYP for CNDO, MNDO, RM1 and PM3 Hamiltonians.

potential range. The values of corrosion current densities in the absence ($i_{corr}$) and presence of inhibitor ($i_{inh}$) were used to estimate the inhibition efficiency from polarization data ($IE_i\%$) using Eq. (5) and the results are also presented in Table 3 [25]

$$IE_i\% = \left(1 - \frac{i_{inh}}{i_{corr}}\right) \times 100 \tag{5}$$

*Adsorption study*

The nature of interaction between the corroding surface of the metal during corrosion inhibition can be explained in terms of the adsorption characteristics of the inhibitor. In this study, results obtained for degree of surface coverage at 303 and 333 K were fitted to a series of different adsorption isotherms including Flory–Huggins, Langmuir, Freundlich and Temkin isotherms. The tests revealed that Langmuir adsorption model best described the adsorption characteristics of the studied purines [26]

$$\frac{C}{\theta} = C + \frac{1}{b_{ads}} \tag{6}$$

where $k$ is the adsorption equilibrium constant, $C$ is the concentration of inhibitor and $\theta$ is the degree of surface coverage of the inhibitor. From the logarithm of both sides of Eqs. (6) and (7) was obtained,

$$log\left(\frac{C}{\theta}\right) = log\, C - log\, b_{ads} \tag{7}$$

By plotting values of $log(C/\theta)$ versus values of $log\, C$, straight line graphs were obtained as shown in Fig. 5 while adsorption parameters deduced from the isotherms are presented in Table 4. From the results obtained, $R^2$ values ranging from 0.9972 to 1.000 were obtained. This indicated a high degree of fitness of the adsorption data to the Langmuir model. However, values obtained for slopes were less than unity indicating the existence of interaction between the adsorbed species and that some components of GU, AD and HPY molecules will occupy more than one adsorption sites on the Al surface [27]. Therefore, Flory Huggins and El Awardy et al. isotherms were also used to explain the existence of interaction.

Flory–Huggins adsorption models consider that prior to adsorption, some molecules of water must be replaced by corresponding molecules of the inhibitor such that the following equilibrium (Eq. (8)) is established [28],

$$A_{soln} + n(H_2O)_{ads} = A_{ads} n(H_2O)_{soln} \tag{8}$$

$$\frac{\theta}{(1-\theta)^n} = b_{ads} C \tag{9}$$

where $n$ is the number of adsorption site. From Eq. (8), Flory Huggins derived an adsorption model expressed by Eq. (9). The main characteristic of the above isotherm is the appearance of the term, $\theta/(1-\theta)^n$ in the expression. From the logarithm and rearrangement of Eqs. (9) and (10) was obtained,

$$log\left(\frac{\theta}{C}\right) = log\, b_{ads} + n log(1-\theta) \tag{10}$$

Fig. 6 shows the Flory–Huggins plots for the adsorption of AD, GU and HPY on Al surface at 303 and 333 K. Adsorption parameters deduced from the plots are also presented in Table 4. From the results obtained, it can be seen that the

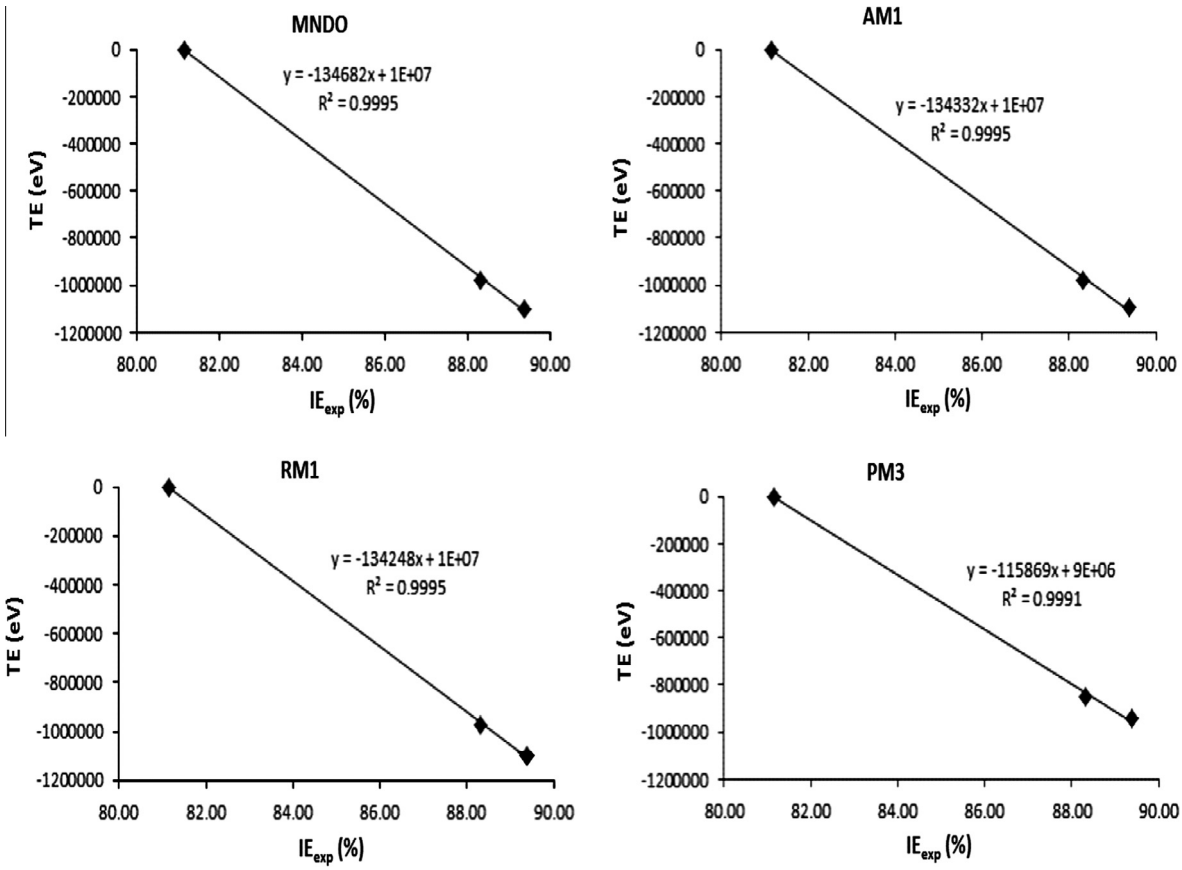


**Fig. 9** Variation of TE with experimental inhibition efficiencies of ADN, GUN and HYP for MNDO, AM1, RM1 and PM3 Hamiltonians.

numerical values of n change from 1 to 2, 1 to 4 and 2 to 3 for AD, GU and HPY at 303 and 333 K, respectively. These changes indicated that the number of water molecules that must be replaced by the respective inhibitor's molecule increases with increase in temperature supporting the formation of multi-molecular layer of adsorption as the temperature increases from 303 to 333 K.

The strength of adsorption of AD, GU and HPY on the surface of Al and the possibility of formation of multi-molecular layer of adsorption were also investigated using the El-Awady et al. kinetic isotherm, which can be written as Eq. (11) [29],

$$\log\left(\frac{\theta}{1-\theta}\right) = \log b' + y\log C \tag{11}$$

where $y$ is the number of inhibitor molecules occupying one active site and $1/y$ represents the number of active sites on the surface occupied by one molecule of the inhibitor. '$y$' is also related to the binding constant, $B$ through $B = b^{(1/y)}$. Fig. 7 shows El-Awady et al., isotherm for the adsorption of the studied purines while adsorption parameters deduced from the isotherm are also presented in Table 4. The results obtained reveal that values of $1/y$ are less than unity confirming that a given inhibitor's molecules will occupy more than one active site (i.e. $1/y < 1$). Also, $B$ values were found to increase with temperature. Generally, larger value of the binding constant ($B$) implies better adsorption arising from stronger electrical interaction between the double layer existing at the phase boundary and the adsorption molecule. On the other hand, small values of the binding constant suggest weaker interaction between the adsorbing molecules and the metal surface. Therefore, the extent of adsorption of AD, GU and HPY on Al surface increases with temperature,

The equilibrium constant of adsorption ($b_{ads}$) obtained from the adsorption models, is related to the standard free energy of adsorption $\Delta G^0_{ads}$ according to Eq. (12) [30]:

$$b_{ads} = \frac{1}{55.5} exp\left(\frac{\Delta G^0_{ads}}{RT}\right) \tag{12}$$

where $R$ is the molar gas constant, $T$ is the absolute temperature and 55.5 is the molar concentration of water in the solution. Values of $\Delta G^0_{ads}$ calculated from Eq. (12) are also presented in Table 4. From the results obtained, the free energies are negatively less than the threshold value (−40 kJ/mol) expected for the mechanism of chemical adsorption hence the adsorption of AD, GU and HPY on Al surface is consistent with electrostatic interactions between the inhibitors' molecules and charged metal surface, which support physisorption mechanism [31].

*Effect of temperature*

The adsorption of an organic inhibitor can affect the corrosion rate by either decreasing the available reaction area (geometric

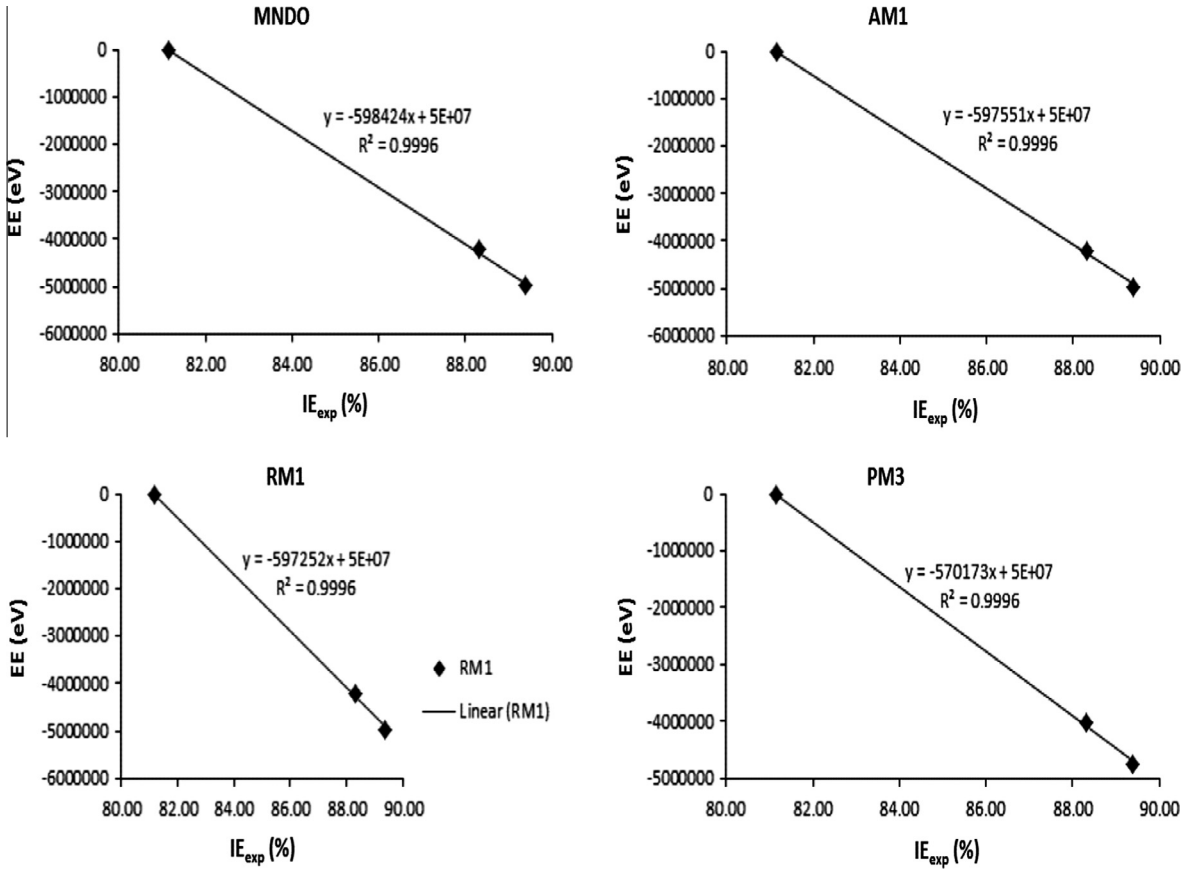


**Fig. 10** Variation of EE with experimental inhibition efficiencies of ADN, GUN and HYP for MNDO, AM1, RM1 and PM3 Hamiltonians.

blocking effect) or by modifying the activation energy of the anodic or cathodic reactions occurring in the inhibitor-free surface in the course of the inhibited corrosion process. The adsorption mechanism of AD, GU and HYP onto aluminum was investigated by changing the temperature of the systems from 303 to 333 K. The apparent activation energies ($E_a$) for the corrosion process in the absence and presence of AD, GU and HYP were calculated using a modified form of the Arrhenius equation [32]:

$$log\frac{CR_1}{CR_2} = \frac{E_a}{2.303R}\left(\frac{1}{T_1} - \frac{1}{T_2}\right) \quad (13)$$

where $CR_1$ and $CR_2$ are the corrosion rates at temperatures $T_1$ and $T_2$, respectively. Calculated values of $E_a$ are presented in Table 5. The activation energies are higher in inhibited HCl solutions compared to the uninhibited system (blank). This is frequently interpreted as being suggestive of formation of an adsorption film of physical/electrostatic nature [33].

The heat of adsorption ($Q_{ads}$) was quantified from the trend of surface coverage with temperature using the following equation [34]:

$$Q_{ads} = 2.303R\left[log\left(\frac{\theta_2}{1-\theta_2}\right) - log\left(\frac{\theta_1}{1-\theta_1}\right)\right] \times \frac{T_1T_2}{T_2 - T_1} \quad (14)$$

where $\theta_1$ and $\theta_2$ are the degrees of surface coverage at temperatures $T_1$ and $T_2$, and $R$ is the gas constant. Negative $Q_{ads}$ values were obtained for the inhibition behavior of AD, GU and HYP (Table 5). This implies that the inhibition of Al corrosion by the studied purines is exothermic and that their inhibition efficiencies decreased with increase in temperature (see Table 1) which is a good indication of a physisorptive kind of interaction between these purines and the metal surfaces.

## Quantum chemical study

### *Global reactivity*

Quantum chemical principles have been widely used to study corrosion inhibition including structure optimization calculations, semi-empirical, ab initio and DFT calculations. In this study, calculated values of semi-empirical parameters for different Hamiltonians (namely, CNDO, MNDO, AM1, RM1 and PM3) were correlated with experimental inhibition efficiencies, while Fukui functions were used to study electrophilic substitution within the inhibitors.

Table 5 presents values of the frontier molecular orbital energies (i.e. energy of the highest occupied molecular orbital ($E_{HOMO}$), energy of the lowest unoccupied molecular orbital ($E_{LUMO}$) and the energy gap ($E_{L-H}$)), total energy (TE), electronic energy (EE), core core interaction energy (CCR) and dipole moment ($\mu$). Figs. 8–11 present plots for the variation of $E_{L-H}$, TE, EE and $E_b$ with experimental inhibition efficiencies of the studied inhibitors. $E_{HOMO}$ indicates the tendency of an inhibitor to donate electron while $E_{LUMO}$ is

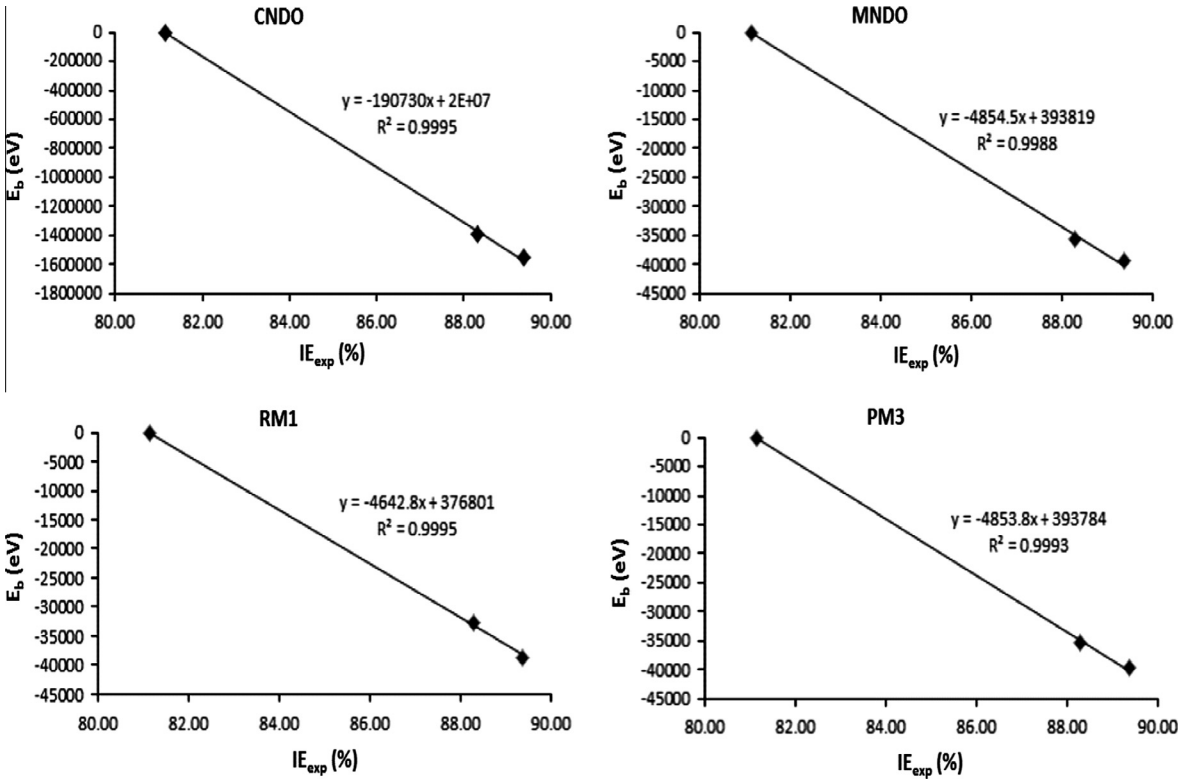


**Fig. 11** Variation of $E_b$ with experimental inhibition efficiencies of ADN, GUN and HYP for CNDO, MNDO, RM1 and PM3 Hamiltonians.

an index that indicate the tendency of a molecular specie to accept electron. The difference between $E_{\mathrm{LUMO}}$ and $E_{\mathrm{HOMO}}$ is the energy gap (i.e. $E_{\mathrm{L-H}}$). In view of this, corrosion inhibition efficiency is expected to increase with increasing values of $E_{\mathrm{HOMO}}$ and with increase in the value of $E_{\mathrm{LUMO}}$ and that of the energy gap. Correlations between calculated values of $E_{\mathrm{HOMO}}$ and experimental inhibition efficiencies were very poor and $R^2$ were lower than 0.45 for all the Hamiltonian considered. Similarly, calculated values of $E_{\mathrm{LUMO}}$ did not correlate significantly with values of experimental inhibition efficiencies. This observation suggests that the inhibition efficiencies of the studied purines are not affected by electron transfer process, a mechanism that favors physical adsorption as proposed earlier. On the other hand, better correlation was obtained between $E_{\mathrm{L-H}}$ and experimental inhibition efficiencies of the studied purines. Generally, the energy gap of a molecule is a quantum chemical parameter that indicates hardness or softness of molecular specie. Hard molecules are characterized with larger value of energy gap and are less reactive than soft molecules, which are characterize by small energy gap [35]. Therefore, corrosion inhibition potential of a molecule is expected to increase with decreasing value of $E_{\mathrm{L-H}}$ as observed in the present study. Although PM3 Hamiltonian did not give excellent correlation between experimental inhibition efficiency with $E_{\mathrm{L-H}}$, calculated values of $R^2$ for CNDO, MNDO, AM1 and RM1 Hamiltonians were within the range of 0.7297 and 0.8155 indicating better relationship between $E_{\mathrm{L-H}}$ and the measured inhibition efficiency (Fig. 8). Excellent correlations were also found between experimental inhibition efficiency and TE and also for EE and $E_b$ (Figs. 9–11). Correlations between $\mathrm{IE_{exp}}$ and TE were excellent for MNDO, AMI, RM1 and PM3 Hamiltonians as indicated in the plots (Fig. 9). Similarly, excellent correlations were found for MNDO, AM1, RM1 and PM3 Hamiltonians with respect to the variation of $\mathrm{IE_{exp}}$ and EE of the molecules. However, AM1 Hamiltonian did not give excellent correlation between $\mathrm{IE_{exp}}$ and $E_b$. Since each Hamiltonians is based on specific assumption, it can be stated that the failure of some of these assumptions for some molecules can lead to poor correlation.

Ionization energy and electron affinity of the inhibitors were calculated using the method of finite difference approximation as follows [36],

$$\mathrm{IE} = E_{(N-1)} - E_{(N)} \tag{15}$$

$$\mathrm{EA} = E_{(N)} - E_{(N+1)} \tag{16}$$

where IE and EA are ionization energy and electron affinity respectively, $E_{(N-1)}$, $E_{(N)}$ and $E_{(N+1)}$ are the ground state energies of the system with $N-1$ and $N+1$ electrons respectively. Calculated values of IE and EA are presented in Table 6. Correlation between $\mathrm{IE_{exp}}$ and IE and between $\mathrm{IE_{exp}}$ and EA were excellent ($R^2$ ranged from 0.79 to 0.89). Also, strong correlations were obtained between IE and $E_{\mathrm{HOMO}}$ and between EA and $E_{\mathrm{LUMO}}$ indicating that IE is associated with the tendency of the inhibitor to donate electron while EA is associated with the tendency of the inhibitors to accept electron. Similar findings have been reported by other researchers [37]. The global hardness which is the inverse of the global softness (i.e. $\eta = 1/S$) can be evaluated using Eq. (17),

**Table 6** Some quantum chemical descriptors for AD, GU and HPY.

| Inhibitor | Hamiltonian | IE (eV) | EA (eV) | $S$ | $\eta$ (eV) | $\chi$ (eV) | $\delta$ |
|---|---|---|---|---|---|---|---|
| HYP | CNDO | 10.9662 | −2.0136 | 0.0770 | 12.9798 | 6.4899 | −0.0128 |
| | MNDO | 9.4434 | −0.1960 | 0.1037 | 9.6394 | 4.8197 | 0.0694 |
| | AM1 | 9.4234 | −0.2467 | 0.1034 | 9.6701 | 4.8351 | 0.0684 |
| | RM1 | 9.3801 | 0.9197 | 0.1182 | 8.4604 | 4.2302 | 0.1140 |
| | PM3 | 9.1975 | −0.4223 | 0.1040 | 9.6198 | 4.8099 | 0.0701 |
| QU | CNDO | 9.1143 | −2.4394 | 0.0866 | 11.5537 | 5.7769 | 0.0165 |
| | MNDO | 8.5389 | −0.2467 | 0.1138 | 8.7856 | 4.3928 | 0.1005 |
| | AM1 | 8.4968 | 0.0251 | 0.1180 | 8.4717 | 4.2358 | 0.1135 |
| | RM1 | 8.3759 | 0.0642 | 0.1203 | 8.3117 | 4.1558 | 0.1205 |
| | PM3 | −4.8242 | 13.2261 | −0.0554 | −18.0503 | −9.0252 | −0.4206 |
| AD | CNDO | 10.1571 | −2.7802 | 0.0773 | 12.9373 | 6.4687 | −0.0120 |
| | MNDO | 9.1715 | −1.1005 | 0.0974 | 10.2720 | 5.1360 | 0.0498 |
| | AM1 | 8.9903 | −0.7983 | 0.1022 | 9.7885 | 4.8943 | 0.0646 |
| | RM1 | 8.1140 | −0.6235 | 0.1144 | 8.7375 | 4.3687 | 0.1024 |
| | PM3 | 8.4825 | −0.3308 | 0.1135 | 8.8134 | 4.4067 | 0.0994 |

**Table 7** Milliken charges of GU, AD and HPY radical ($N$), cation ($N-1$) and anion ($N+1$) calculated from DFT.

| Atom no. | $N$ | $N-1$ | $N+1$ | $N$ | $N-1$ | $N+1$ | $N$ | $N-1$ | $N+1$ |
|---|---|---|---|---|---|---|---|---|---|
| 1 | −0.7902 | −0.7589 | −0.8082 | −0.7660 | −0.7341 | −0.7915 | −0.5819 | −0.5061 | −0.6562 |
| 2 | 0.2771 | 0.3325 | 0.1718 | 0.2733 | 0.3244 | 0.1761 | 0.2015 | 0.2458 | 0.1719 |
| 3 | −0.5039 | −0.4366 | −0.5719 | −0.5251 | −0.4609 | −0.5798 | −0.5401 | −0.4290 | −0.6267 |
| 4 | 0.4495 | 0.5163 | 0.3833 | 0.4391 | 0.4784 | 0.3539 | 0.4080 | 0.4416 | 0.3438 |
| 5 | −0.5341 | −0.4344 | −0.6306 | −0.6336 | −0.5295 | −0.6736 | 0.2737 | 0.3327 | 0.2470 |
| 6 | 0.1986 | 0.2895 | 0.1636 | 0.8830 | 0.9417 | 0.8213 | 0.6021 | 0.6408 | 0.5002 |
| 7 | −0.5637 | −0.4845 | −0.6381 | −0.7965 | −0.7318 | −0.8196 | −0.7857 | −0.6776 | −0.8196 |
| 8 | 0.6477 | 0.7381 | 0.5186 | −0.8149 | −0.8037 | −0.8267 | −0.4961 | −0.4242 | −0.5629 |
| 9 | −0.5898 | −0.5137 | −0.6474 | 0.6750 | 0.7290 | 0.5698 | 0.2766 | 0.3166 | 0.1733 |
| 10 | 0.2463 | 0.3025 | 0.2252 | −0.5217 | −0.3956 | −0.6328 | −0.7631 | −0.7213 | −0.7845 |
| 11 | | | | 0.0.2485 | 0.3283 | 0.2080 | | | |

**Table 8** Condensed Fukui functions for AD, GU and HPY calculated from Milliken charges using DFT.

| Atom no. | HPY | | GU | | AD | |
|---|---|---|---|---|---|---|
| | $f_k^+$ | $f_k^+$ | $f_k^+$ | $f_k^+$ | $f_k^+$ | $f_k^{+-}$ |
| 1 | −0.0180 | −0.0313 | −0.0255 | −0.0319 | −0.0742 | −0.0759 |
| 2 | −0.1053 | −0.0554 | −0.0972 | −0.0512 | −0.0296 | −0.0443 |
| 3 | −0.0680 | −0.0673 | −0.0547 | −0.0642 | −0.0867 | −0.1111 |
| 4 | −0.0662 | −0.0668 | −0.0852 | −0.0394 | −0.0643 | −0.0336 |
| 5 | −0.0965 | −0.0997 | −0.0401 | −0.1041 | −0.0267 | −0.0590 |
| 6 | −0.0350 | −0.0909 | −0.0617 | −0.0588 | −0.1019 | −0.0387 |
| 7 | −0.0744 | −0.0792 | −0.0231 | −0.0647 | −0.0339 | −0.1081 |
| 8 | −0.1291 | −0.0904 | −0.0118 | −0.0112 | −0.0669 | −0.0719 |
| 9 | −0.0575 | −0.0762 | −0.1053 | −0.0540 | −0.1033 | −0.0400 |
| 10 | −0.0212 | −0.0562 | −0.1111 | −0.1261 | −0.0214 | −0.0418 |
| 11 | | | −0.0405 | −0.0798 | | |

$$S = \frac{1}{[(E_{(N-1)} - E_{(N)} - (E_{(N)} - E_{(N+1)})]} \tag{17}$$

where $S$ is the global softness and $\eta$ is the global harness. Calculated values of $S$ and $\eta$ are also presented in Table 6. Although calculated values of $S$ and $\eta$ did not show strong correlation with the experimental inhibition efficiencies ($R^2 = 0.589$ and 0.657 respectively), correlations between these parameters and $E_{L-H}$ were strong indicating that $S$ and $\eta$ are related to $E_{L-H}$ which is an index for measuring the softness of a molecule.

The fraction of electron transferred, $\delta$ can be calculated using Eq. (18) [38],

$$\delta = \frac{(\chi_{Al} - \chi_{inh})}{(\eta_{Al} + \eta_{inh})} \tag{18}$$

**Table 9** Huckel charges and condensed Fukui functions for GU calculated from Milliken and Lowdin charges using MP2 level of theory.

| Atom and atom number | Huckel charge | Milliken | | Lowdin | |
|---|---|---|---|---|---|
| | | $f_k^+$ | $f_k^-$ | $f_k^+$ | $f_k^-$ |
| N(1) | 0.2591 | −0.0370 | 0.0048 | −0.0613 | 0.0219 |
| C(2) | 0.1757 | −0.0674 | 0.0180 | −0.1075 | 0.0323 |
| N(3) | −0.5442 | 0.0079 | −0.1262 | 0.0372 | −0.1346 |
| C(4) | 0.2082 | −0.1063 | 0.0433 | −0.1192 | 0.0434 |
| N(5) | −0.5898 | −0.0672 | −0.1977 | −0.0705 | −0.2581 |
| C(6) | 0.3965 | −0.0376 | −0.0576 | −0.0235 | −0.0526 |
| N(7) | 0.0237 | −0.0208 | −0.0533 | −0.0250 | −0.0719 |
| N(8) | 0.2467 | −0.0004 | −0.0422 | −0.0292 | −0.0515 |
| C(9) | 0.4078 | −0.2194 | 0.0627 | −0.2545 | 0.1051 |
| O(10) | −0.8803 | −0.1562 | −0.2689 | −0.1693 | −0.3117 |
| C(11) | −0.0993 | 0.0386 | −0.1307 | 0.0569 | −0.1385 |

**Table 10** Huckel charges and condensed Fukui functions for AD calculated from Milliken and Lowdin charges using MP2 level of theory.

| Atom and atom number | Huckel charge | Milliken | | Lowdin | |
|---|---|---|---|---|---|
| | | $f_k^+$ | $f_k^-$ | $f_k^+$ | $f_k^-$ |
| N(1) | −0.5113 | −0.0769 | −0.0716 | −0.0841 | −0.0577 |
| C(2) | 0.2450 | −0.0286 | −0.1250 | −0.0402 | −0.1479 |
| N(3) | −0.3972 | −0.0658 | −0.1378 | −0.0584 | −0.2491 |
| C(4) | 0.1554 | −0.0116 | −0.0552 | 0.0161 | −0.0348 |
| C(5) | −0.0362 | −0.0552 | −0.0397 | −0.0587 | −0.0249 |
| C(6) | 0.3228 | −0.0495 | −0.0680 | −0.0433 | −0.0767 |
| N(7) | −0.0216 | −0.0168 | −0.0369 | −0.0211 | −0.0498 |
| N(8) | −0.4966 | −0.1472 | −0.0482 | −0.1892 | −0.0315 |
| C(9) | 0.1837 | −0.1299 | −0.0509 | −0.1957 | −0.0621 |
| N(10) | 0.2447 | −0.0163 | −0.0241 | −0.0567 | −0.0303 |

**Table 11** Huckel charges and condensed Fukui functions for HPY calculated from Milliken and Lowdin charges using MP2 level of theory.

| Atom and atom number | Huckel charge | Milliken | | Lowdin | |
|---|---|---|---|---|---|
| | | $f_k^+$ | $f_k^-$ | $f_k^+$ | $f_k^-$ |
| N(1) | 0.2471 | −0.0166 | −0.0401 | −0.0447 | −0.0594 |
| C(2) | 0.2316 | −0.1389 | −0.0396 | −0.2119 | −0.0499 |
| N(3) | −0.5196 | −0.1297 | −0.0810 | −0.1636 | −0.0671 |
| C(4) | 0.2621 | −0.0249 | −0.0320 | −0.0016 | −0.0235 |
| N(5) | −0.4258 | −0.1048 | −0.0867 | −0.1223 | −0.0911 |
| C(6) | 0.2277 | −0.0254 | −0.0904 | −0.0318 | −0.1241 |
| N(7) | −0.3770 | −0.0738 | −0.0389 | −0.0788 | −0.0177 |
| C(8) | 0.3372 | −0.0945 | −0.1278 | −0.0996 | −0.1486 |
| O(9) | −0.2551 | −0.0426 | −0.0776 | −0.0410 | −0.0812 |
| C(10) | −0.0292 | −0.0053 | −0.0815 | 0.0206 | −0.1285 |

where $\chi_{Al}$ and $\chi_{inh}$ are the electronegativities of Al and the inhibitor respectively and can be evaluated as $\chi = (IP + EA)/2$. $\eta_{Al}$ and $\eta_{inh}$ are the global hardness of Al and the inhibitor respectively. Calculated values of $\delta$ are also presented in Table 6. $\delta$ values did not correlate strongly with the experimental inhibition efficiencies of the inhibitors and were relatively low, indicating that fewer electrons were transferred from the inhibitor to the metal surface. Therefore, the inhibition of the corrosion of aluminum by AD, GU and HYP supports the transfer of charge or electron from the inhibitor to the metal surface indicating the occurrence of physical and chemical adsorption mechanism. However, physical adsorption mechanism precedes chemisorption mechanism.

*Local reactivity*

In this study, local reactivity was investigated using the Fukui functions deduced through DFT and MP2 calculations. The Fukui function has been formally defined as

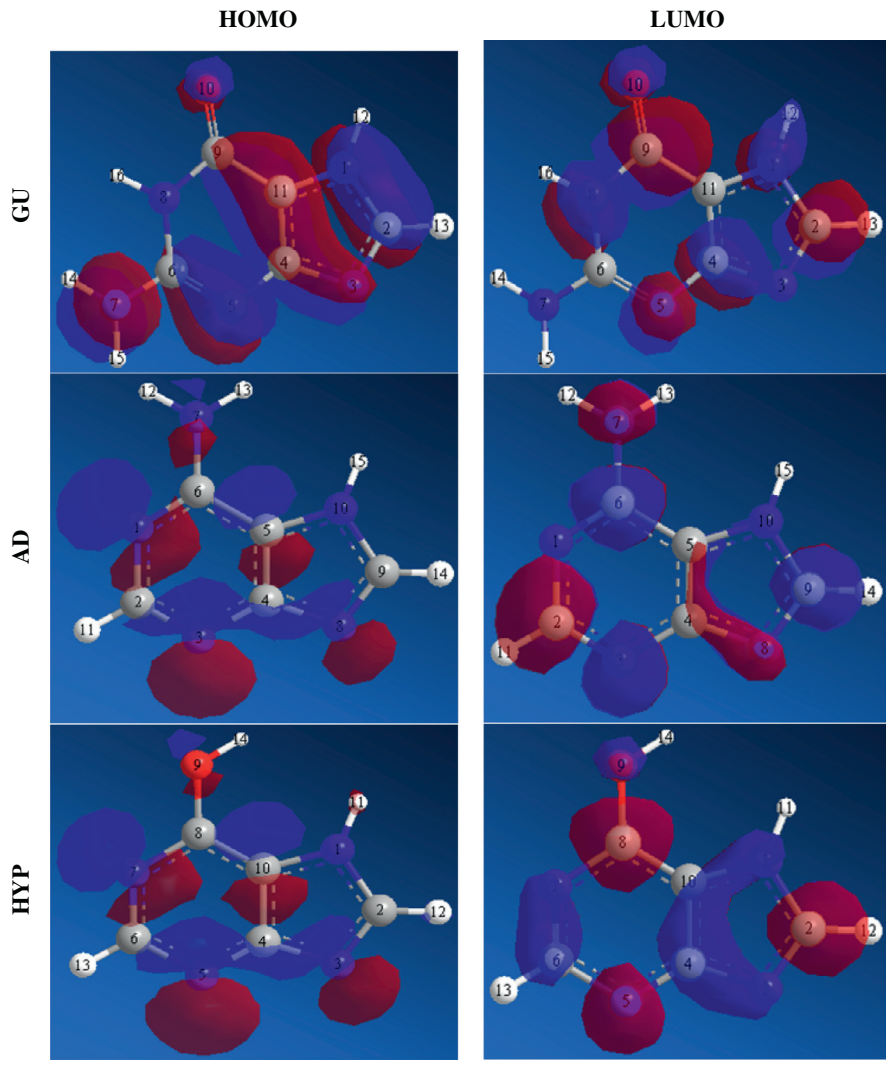


**Fig. 12** HOMO and LUMO molecular orbitals of AD, GU and HPY.

$$f(r) = \left[\frac{\delta\mu}{\delta v(r)}\right]_N \tag{19}$$

where $v(r)$ is the external potential and the functional derivatives must be taken at constant number of electrons. Assuming that the total energy $E$ as a function of $N$ and functional of $v(r)$ is an exact differential, the Maxwell relations between derivatives may be applied to write

$$f(r) = \left(\frac{\delta\rho(r)}{\delta N}\right)_v \tag{20}$$

Eq. (20) is the most standard presentation of the Fukui function. Owing to the discontinuity of the chemical potential at integer $N$, the derivative will be different if taken from the right or the left side. Therefore, there are three different functions, $f^+(r)$ (corresponding to the situation when the derivative is taken as $N$ increases from $N$ to $N + \delta$), $f^-(r)$ corresponding to a situation when $N$ decreases to $N - \delta$) and $f^0(r)$ the average of the two. In practice, condensed Fukui function is often used and are defined as follows,

$$f_k^- = q_k(N) - q_k(N-1) \tag{21}$$

$$f_k^+ = q_k(N+1) - q_k(N) \tag{22}$$

In this work, condensed Fukui functions were calculated using Huckel and Muliken charges at DFT and MP2 level of theories. Values of Mulliken charges and Fukui functions calculated for DFT level of theories using Muliken charges are presented in Tables 7 and 8 respectively. Fukui functions computed for MP2 level of theory using Muliken and Lowdin charges are also presented in Tables 9–11. From the results obtained, values of condensed Fukui functions were negative indicating unphysical results [39]. Therefore, calculation of the binding energies between Al and the inhibitors, for the various positions of hetero atoms was carried out.

The interaction energy between the inhibitor and the aluminum atom can be calculated using Eq. (23) [40],

$$E_{\text{int}} = E_{(\text{Al}-X)} - (E_x + E_{\text{Al}}) \tag{23}$$

where $E_{\text{Al}}$ is the total energy of the iron atom, $E_x$ is the total energy of inhibitory compound and $E_{(\text{Al}-\text{X})}$ is the energy of interaction between aluminum and the inhibitor. When absorption occurs between the compound and the aluminum atom, the energy of the new system is expressed as $E_x + E_{\text{Al}}$. Table 12 shows the binding energies for various positions of the hetero atoms in AD, GU and HPY respectively. Since every systems prefer to remain in states of lowest energy, it can be stated that in GU the

**Table 12** Binding energies for various positions of hetero atoms in AD, GU and HPY.

| Inhibitor | Atom | $E_{(Al-X)}$ (J/mol) | $E_{inh} + E_{Al}$ (J/mol) | $E_{int}$ (J/mol) |
|---|---|---|---|---|
| GU | N1 | 18.433 | 18.376 | 0.057 |
| | N3 | 13.156 | 18.376 | −5.22 |
| | N5 | 17.266 | 18.376 | −1.11 |
| | N7 | 18.531 | 18.376 | 0.155 |
| | O10 | 16.714 | 18.376 | −1.662 |
| AD | N1 | 17.202 | 19.061 | −1.859 |
| | N3 | 17.786 | 19.061 | −1.275 |
| | N7 | 18.992 | 19.061 | −0.069 |
| | N8 | 13.056 | 19.061 | −6.005 |
| | N10 | 20.081 | 19.061 | 1.02 |
| HPY | N1 | 21.895 | 20.294 | 1.601 |
| | N3 | 15.206 | 20.294 | −5.088 |
| | N5 | 18.204 | 20.294 | −2.09 |
| | N7 | 19.122 | 20.294 | −1.172 |
| | O9 | 22.539 | 20.294 | 2.245 |

adsorption of the inhibitor (hence inhibition mechanism) occurred in the imine nitrogen (i.e. N5), in AD, the adsorption site is emanine nitrogen (i.e. N7) and in HPY, the adsorption site is in the pyridine nitrogen (i.e. N5). Considerations of Huckel charges for these sites (Tables 9–11) also revealed that these sites possess reasonable negative charges that can interact with the charged metal (Al) surface. Since inhibition efficiency of an inhibitor is closely related to the strength of adsorption, it can be stated that the listed adsorption sites enhances the efficiencies of the studied purines due to the high concentration of electrons. Hence the HOMO and LUMO molecular orbital of AD, GU and HPY are produced in Fig. 12. It is significant to note that the LUMO corresponds to $f^{+}(r)$ (i.e. tendency to accept electron) while the HOMO corresponds to $f^{-}(r)$ (i.e. tendency to donate electron). Therefore, the nature and distribution of the lopes in the HOMO and LUMO diagrams (Fig. 12) also support the findings deduced from the interaction energies and from Huckel charges (Table 12).

## Conclusions

From the results and findings of this study, the following conclusions were made,

i. AD, GU and HPY are excellent corrosion inhibitors for the corrosion of Al in acidic medium.
ii. The inhibitors are adsorption inhibitors and their adsorptions on Al surface were spontaneous and were consistent with physiosorption mechanism. The adsorption behavior of the inhibitors supported the models of Flory Huggins, Langmuir and El Awardy et al.
iii. Inhibition efficiencies of AD, GU and HPY strong correlations with some quantum chemical parameters. Fukui functions at DFT and MP2 levels of theory are unphysical in predicting the sites for electrophilic and nucleophilic attacks but considerations of interaction energies between Al and various sites of the hetero atoms revealed likely adsorption sites.

## Conflict of interest

*The authors have declared no conflict of interest.*

## Compliance with Ethics Requirements

*This article does not contain any studies with human or animal subjects.*

## References

[1] Fouda AS, Gouda MM, Abd El-Rahman SI. Benzaldehyde, 2-hydroxybenzoyl hydrazone derivatives as inhibitors of the corrosion of aluminium in hydrochloric acid. Chem Pharm Bull 2000;48:636–40.
[2] Cabot PL, Centellas FA, Garrido JA, Perez E, Vidal H. Electrochemical study of aluminium corrosion in acid chloride solutions. Electrochim Acta 1991;36:171–87.
[3] Al-Kharafi FM, Badawy WA. Inhibition of corrosion of Al 6061, aluminum, and an aluminum–copper alloy in chloride-free aqueous media: Part 2—Behavior in basic solutions. Corrosion 1998;54:377–85.
[4] Srinivasan HS, Mital CK. Studies on the passivation behavior of Al–Zn–Mg alloy in chloride solutions containing some anions and cations using electrochemical impedance spectroscopy. Electrochim Acta 1994;39:2633–7.
[5] Lin CS, Chiu CC. Formation of the layered etch films on AA1050 aluminum plates etched in nitric acid using alternating currents. J Electrochem Soc 2005;152:482–7.
[6] Ameh PO, Eddy NO. *Commiphora pedunculata* gum as a green inhibitor for the corrosion of aluminium. Res Chem Intermed 2014;40(8):2641–9.
[7] Eddy NO, Ameh PO, Gimba CE, Ebenso EE. Rheological modeling and characterization of *Ficus platyphylla* gum exudates. J Chem 2013. http://dx.doi.org/10.1155/2013/254347.
[8] Eddy NO. Experimental and theoretical studies on some amino acids and their potential activity as inhibitors for the corrosion of mild steel, Part 2. J Adv Res 2011;2:35.
[9] Elayyoubi SB, Hammouti S, Kertit HO, Maarouf EB. Corrosion inhibition of mild steel in hydrochloric acid solutions by malonitrile compounds. Rev Met Paris 2004;2:153–7.
[10] Okafor PC, Osabor V, Ebenso EE. Eco friendly corrosion inhibitors: Inhibitive action of ethanol extracts of *Garcinia kola* for the corrosion of aluminium in acidic medium. Pig Resin Technol 2007;36(5):299–305.
[11] Bilgic L, Caliskan N. An investigation of some Schiff bases as corrosion inhibitors for austenite chromium–nickel steel in $H_2SO_4$. J Appl Electrochem 2001;52(31):79–83.

[12] El Ashry EH, El Nemr A, Essawy SA, Ragab S. Corrosion inhibitors Part III: Quantum chemical studies on the efficiencies of some aromatic hydrazides and Schiff bases as corrosion inhibitors of steel in acidic medium. ARKIVOC 2006;11:205–20.
[13] Emergull KC, Kurtaran R, Atakol O. An investigation of chloride-substituted Schiff bases as corrosion inhibitors for steel. J Corros Sci 2003;45:2803–17.
[14] Li X, Deng S, Fu H, Li T. Adsorption and inhibition effect of 6-benzylaminopurine on cold rolled steel in 1.0 M HCl. Electrochim Acta 2009;54:4089–98.
[15] Scendo M. The effect of purine on the corrosion of copper in chloride solutions. Corros Sci 2007;49:373–90.
[16] Scendo M. Inhibitive action of purine and adenine for copper corrosion in sulphate solutions. Corros Sci 2007;49:2985–3000.
[17] Scendo M. The influence of adenine on corrosion of copper in chloride solutions. Corros Sci 2008;50:2070–7.
[18] Yan Y, Weihua L, Lankun C, Baorong H. Electrochemical and quantum chemical study of purines as corrosion inhibitors for mild steel in 1 M HCl solution. Electrochim Acta 2008;53:5953–60.
[19] Habibat M, Eddy NO, Iyun J, Gimba CE, Oguzie E. Hypoxanthine as an inhibitor for mild steel corrosion in 0.1 M HCl. Chem Mater Res 2012;2(4):1–12.
[20] Khaled KF. Electrochemical investigation and modeling of corrosion inhibition of aluminum in molar nitric acid using some sulphur-containing amines. Corros Sci 2010:2905–16.
[21] Lukovitis L, Shaban A, Kalman E. Corrosion inhibitor, quantitative structural activity relationships. Russ J Electrochem 2003;19(2):177–81.
[22] Oguzie EE, Enenebeaku CK, Akalezi CO, Okoro SC, Ayuk AA, Ejike EN. Adsorption and corrosion inhibiting effect of *Dacryodis edulis* extract on low carbon steel corrosion in acidic media. J Colloid Interf Sci 2010;349:283–92.
[23] Abdallah M. Guar gum as corrosion inhibitor for carbon steel in sulfuric acid solutions. Portugaliae Electrochim Acta 2004;22:161–75.
[24] Acharya S, Upadhyay SN. The inhibition of corrosion of mild steel by some fluoroquinolones in sodium chloride solution. Trans Indian Inst Met 2004;57(3):297–306.
[25] Ebadi M, Basirun WJ, Leng SY, Mahmoudian MR. Investigation of corrosion inhibition properties of caffeine on nickel by electrochemical techniques. Int J Electrochem Sci 2012;7:8052–63.
[26] Yadav JK, Maiti B, Quraishi MA. Electrochemical and quantum chemical studies of 3,4-dihydropyrimidin-2(1H)-ones as corrosion inhibitors for mild steel in hydrochloric acid solution. Corros Sci 2010:3586–98.
[27] Eddy NO. Theoretical study on some amino acids and their potential activity as corrosion inhibitors for mild steel in HCl. Mol Simul 2010;35(5):354–63.
[28] Adejo SO, Ekwenchi MM, Momoh F, Odiniya E. Adsorption characterization of ethanol extract of leaves of *Portulaca oleracea* as green corrosion inhibitor for corrosion of mild steel in sulphuric acid aedium. Int J Mod Chem 2012;1(3):125–34.
[29] Gojic M. Adsorption and corrosion inhibitive properties of some organic molecules on iron electrode in sulfuric acid. Corros Sci 2002;43:919–29.
[30] Eddy NO. Adsorption and inhibitive properties of ethanol extract of garcina kola and cola nitida for the corrosion of mild steel in $H_2SO_4$. Pig Res Technol 2010;39(6):347.
[31] Akalezi CO, Enenebaku CK, Oguzie EE. Application of aqueous extracts of coffee senna for control of mild steel corrosion in acidic environments. Int J Ind Chem 2012;3:13–25.
[32] Eddy NO, Ebenso EE. Corrosion inhibition and adsorption properties of ethanol eextract of *Gongronema latifolium* on mild steel in $H_2SO_4$. Pig Res Technol 2010;39(2):77–83.
[33] Popova A, Sokolova E, Raicheva S, Christov M. AC and DC study of the temperature effect on mild steel corrosion in acid media in the presence of benzimidazole derivatives. Corros Sci 2003;45(1):33–58.
[34] Olusola JO, Oluseyi AK, Kehinde OO, Olayinka AO, Oluwatosin JM. Adsorption behaviour of [(4-hydroxy-6-methyl-2-oxo-2hpyran-3-yl)-(4-methoxy-phenyl)-1methyl]-urea on stainless steel in phosphoric media. Portugaliae Electrochim Acta 2009;27(5):591–8.
[35] Bhajiwala HM, Vashi RT. Ethanolamine, diethanolamine and triethanolamine as corrosion inhibitors for zinc in binary acid mixture [$HNO_3$ + $H_3PO_4$]. Bull Electrochem Soc 2001;17:441–8.
[36] Eddy NO, Ita BI. Experimental and theoretical studies on the inhibition potentials of some derivatives of cyclopenta-1,3-diene. Int J Quant Chem 2011;111(14):3456–73.
[37] Eddy NO, Ebenso EE, Ibok UJ. Adsorption, synergistic inhibitive effect and quantum chemical studies of ampicillin (AMP) and halides for the corrosion of mild steel in $H_2SO_4$. J Appl Electrochem 2010;40:445–56.
[38] Eddy NO, Ita BI. Theoretical and experimental studies on the inhibition potentials of aromatic oxaldehydes for the corrosion of mild steel in 0.1 M HCl. J Mol Mod 2011;17:633–47.
[39] Sahin M, Gece G, Karci F, Bilgic S. Experimental and theoretical study of the effect of some heterocyclic compounds on the corrosion of low carbon steel in 3.5% NaCl medium. J Appl Electrochem 2008;38:809–15.
[40] Fuentealba P, Perez P, Contreras R. On the condensed Fukui function. J Chem Phys 2000;113(7):2544–51.